



Direct Strength Approach to Predict the Flexural Strength of Cold-Formed Z-Section Purlins on Sloped Roofs

Ali Parva¹, Michael W Seek²

Abstract

In this study, the strength of cold-formed Z-section purlins is predicted considering the effects of roof slope in real roof systems. The study applies to simple span purlins with torsion restraints at support locations and at paired locations along the length of the member. A previously developed method has shown through comparisons to base tests that when the biaxial bending and torsion stresses are incorporated into the analysis, the Direct Strength Method can accurately predict the strength of a purlin. These stress distributions can deviate substantially from the constrained bending approximation typically assumed in analysis and therefore impacts the local and distortional buckling behavior. The method was modified to represent the system conditions in real roofs and to include roof slope.

The base test is a test intended to represent real roof conditions, however second order stresses can be introduced as a result of the limitations of the test. Real roof systems are not subject to some of these second order effects. Similarly, as slope effects are included in the analysis, biaxial bending and torsion stresses can change significantly relative to the flat roof condition, particularly for flexible standing seam diaphragms. This change in stresses in turn changes the local and distortional buckling behavior of the purlin. Initially, for low slope roofs, the predicted strength increases relative to the flat roof condition. As the roof slope increases and the mid-span of the purlin displaces downslope, the flexural strength of the purlin can be less than the flat roof condition. Using the analytical model developed in this study, the strength of purlins is evaluated at different roof slopes and compared to the “real” flat roof condition.

1. Introduction

Roof systems supported by Z-section purlins have gained popularity because of the purlins provide a high strength to weight ratio. The stability of Z-sections in roof systems depends on a combination of support torsion restraints, diaphragm and torsional restraint provided by the sheathing, and braces provided along the span of the purlin. The purlin should be sufficiently restrained such that deflections and thus second order effects are minimized. Current design practice typically assumes that the braces are sufficient to prevent lateral displacement and thus constrain the purlin to bend in the plane of the web. However, Z-sections will typically fail by

¹ Graduate Research Assistant, Old Dominion University, <aparv001@odu.edu>

² Assistant Professor, Old Dominion University, <mseek@odu.edu>

local buckling, distortional buckling, or lateral torsional buckling before reaching the full elastic constrained bending strength. For standing seam systems, the system must be tested using the standard AISI S908-13 Base Test Method (AISI 2013) to determine the reduced capacity (or Reduction factor) relative to the constrained bending strength.

The Component Stiffness Method is a procedure to predict brace forces that is presented in AISI Design Guide for Cold-Formed Steel Purlin Roof Framing Systems (AISI 2009). Through displacement compatibility between the purlin and the restraining components (diaphragm and external braces) the forces in the braces can be determined. This method can be expanded by superimposing the active forces on the structure with the forces generated in the restraining components. With this superposition of forces, the normal bending and torsion warping stresses can be determined.

Seek et al (2016) demonstrated this use of the Component Stiffness Method to calculate the bending and warping normal stresses in a purlin system with paired torsion braces at the 1/3 points along the span as shown in Figure 1. The study showed that for the torsion bracing system, the cross section stresses deviate substantially from the constrained bending case. The calculated stress distributions were then used to perform a finite strip buckling analysis using CUFSM (Li and Schafer, 2010) to calculate the local and distortional buckling strength. The strength was compared to a series of base tests performed on a range of purlin sizes and showed good correlation.

The study performed by Seek et al was based on a bracing configuration with torsion braces at the third points. The prediction equations have been modified to allow for paired braces at any location along the span since it is customary for the industry to locate paired braces within the interior third of the span. The previous study also demonstrated that there are a number of second order effects that are introduced to a system of purlins when tested according to the Base Test Method. The current study applies to “real” roof systems that are not subject to many of the same second order effects. As the current study applies to real roof systems, the equations have been expanded to incorporate roof slope.

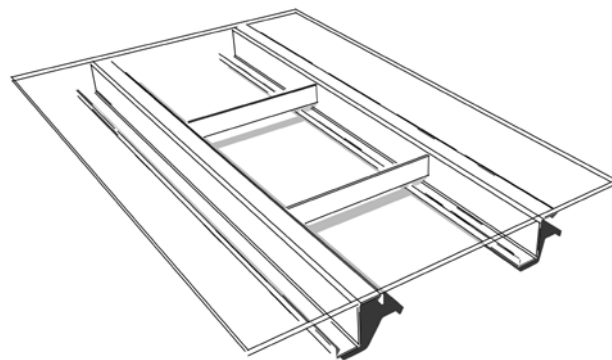


Figure 1. Purlin system with paired torsion braces

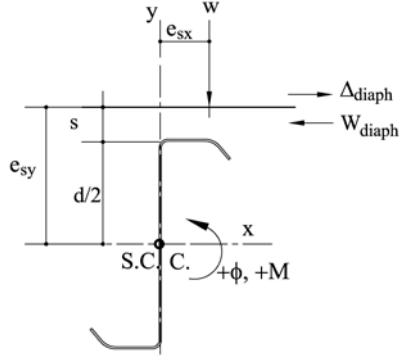


Figure 2. Nomenclature and Positive Load and Displacement Directions

2. Displacement Compatibility of System

Seek et al (2016) presented methods to calculate the forces introduced in the diaphragm for a system that the braces are fixed at the third points on a flat roof purlin system. The method can be further generalized for paired braces placed symmetrically at any point of the span and for roofs at any slope. Previously, the method established displacement compatibility at mid-span. The current method establishes displacement compatibility at the torsion brace location. For a uniform load, w , applied in the direction of gravity on a sloped roof, the uniform force developed in the diaphragm is $w_{rest} = w \cdot \sigma$, where

$$\sigma = \frac{C_1 \left(\frac{I_{xy}}{I_x} \cos \theta \right) L^4 + C_2 \frac{L^2 \sin \theta}{G' spa}}{C_1 \frac{L^4}{EI_{my}} + C_2 \frac{L^2}{G' spa}} \quad (1)$$

and

$$C_1 = \frac{1}{24} \cdot \left(\frac{c}{L} \right) \cdot \left[1 - 2 \left(\frac{c}{L} \right)^2 + \left(\frac{c}{L} \right)^3 \right] \quad (2)$$

$$C_2 = \frac{1}{2} \cdot \left(\frac{c}{L} \right) \cdot \left[1 - \left(\frac{c}{L} \right) \right] \quad (3)$$

G' = stiffness of diaphragm (lb/in)

L = Purlin span

spa = width of diaphragm tributary to the purlin (typically purlin spacing)

$$I_{my} = \frac{I_x I_y - I_{xy}^2}{I_x}$$

θ = roof angle measured from horizontal

c = distance from support location to brace location

Determining the lateral restraint force generated in the diaphragm is crucial because it defines the extent to which a purlin is subjected to biaxial bending, or in other words, deviates from the constrained bending assumption. The in-plane force generated in the diaphragm is proportional to the extent to which the diaphragm constrains the lateral movement of the purlin. If the purlin is perfectly constrained, ie, the diaphragm is perfectly stiff, the term $\sigma = I_{xy}/I_x$. For low slope roofs with a flexible diaphragm, the purlin will deflect in the upslope direction and the term $\sigma < I_{xy}/I_x$. Conversely, for a roof with a steeper slope, the downslope forces will eventually dominate, forcing a downslope deflection of the purlin. As the purlin deflects downslope, $\sigma > I_{xy}/I_x$.

The lateral deflection of the diaphragm at mid-span is defined by Eq. 4. A positive deflection indicates a displacement in the upslope direction and a negative deflection indicates movement in the downslope direction. From Eq. 4 it can be observed that the transition from upslope deflection to downslope deflection occurs when $\sin(\theta) > \sigma$.

$$\Delta_{\text{diaph}} = w(\sigma - \sin \theta) \frac{L^2}{8G'(\text{spa})} \quad (4)$$

Forces are transferred from the diaphragm to the purlin eccentric to the shear center of the purlin. The uniform force perpendicular to the plane of the diaphragm is assumed to act at an eccentricity, e_{sx} , as shown in Fig. 2 equal to one-third the width of the flange. Similarly, the uniform force in the diaphragm acts at an eccentricity, e_{sy} . This eccentricity is equal to half the depth of the flange plus the effective standoff of the clip providing the connection between the purlin and the sheathing. Seek (2017) defines the effective standoff distance and provides approximate values for typical standing seam systems. Combining these two uniform torques, the total uniformly distributed torque along the span of the purlin is

$$t_{1st} = (w)(\sigma \cdot e_{sy} - e_{sx}) \quad (5)$$

As a result of the lateral deflection of the diaphragm relative to the support location, additional second order torsion is introduced to the purlin. This torsion is approximated to have a parabolic distribution, where the peak torsion at mid-span is

$$t_{2nd} = -(w)\Delta_{\text{diaph}} \quad (6)$$

The torsion braces applied along the length of the purlin restrain the deformation caused by the distributed torque along the span. The brace forces are determined such that there is no net rotation at the brace location, ie the torsion braces are infinitely stiff. The torque imparted on the purlin from the first order uniform torsion is

$$T_{1st} = -C_3 t_{1st} L \quad (7)$$

where

$$C_3 = \frac{1}{4} \cdot \frac{1 - 2\left(\frac{c}{L}\right)^2 + \left(\frac{c}{L}\right)^3}{3\left(\frac{c}{L}\right) - 4\left(\frac{c}{L}\right)^2} \quad (8)$$

Similarly, the second order torsion with a parabolic distribution along the span is resisted by the braces, imparting a concentrated torque on the purlin, T_{2nd} , where

$$T_{2nd} = -C_4 t_{2nd} L \quad (9)$$

where

$$C_4 = \frac{1}{15} \cdot \frac{3 - 5\left(\frac{c}{L}\right)^2 + 3\left(\frac{c}{L}\right)^4 - \left(\frac{c}{L}\right)^5}{3\left(\frac{c}{L}\right) - 4\left(\frac{c}{L}\right)^2} \quad (10)$$

Because the torsion brace is only connected to adjacent purlins, for the brace to be in equilibrium, the moments generated at each end of the brace are balanced by shear forces at each end of the brace as shown in Figure 3. The shear forces are equal and opposite at each end and are calculated by.

$$V_i = \frac{2(T_{1st} + T_{2nd})\xi}{spa} \quad (11)$$

Depending on the direction of the torque and the location of the purlin (whether in the upslope or downslope position) the shear force may either increase or decrease the bending moment in the beam. The term ξ accounts for the position of the purlin in the bracing configuration and is (1) for the purlin in the downslope position and (-1) for the upslope position. Note that the calculated shear force will be positive if the shear force acts in the direction of gravity on the purlin.

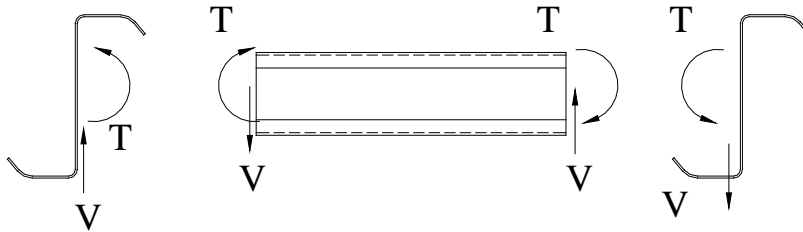


Figure 3 Equilibrium of torsion brace

Bending normal stresses from biaxial and warping torsion can be quantified while having the total moment about the orthogonal x-axis from combined first order and second order bending stresses at any point along the span as:

3. Cross Section Normal Stresses

The various forces determined from displacement compatibility acting on the purlin are superimposed to determine the normal stresses. The two critical locations to investigate are the purlin mid-span and the brace location. With the combination of bending and torsion stresses, it is common for the combination of stresses at the brace location to indicated failure at load levels below which would cause failure at the mid-span. This failure mode commonly occurs in tests of systems with paired torsion braces.

Bending Normal Stresses

The total mid-span moment about the orthogonal x-axis from the combination of the applied uniformly distributed load and the added shear forces in the braces is

$$M_{\text{mid}} = \frac{wL^2}{8} + (V_i)c \quad (12)$$

Similarly, the bending moment at the location of the torsion brace from the combination of loads is

$$M_c = w \frac{c}{2} ((L-c) + (V_i)c) \quad (13)$$

The bending normal stresses from biaxial bending of the cross section are calculated at each point along the cross section defined by coordinates (x,y) by

$$f_b = M \cdot \left[\frac{-y}{I_{mx}} + \frac{x}{I_{my}} - \frac{x \cdot \sigma}{I_{my}} + \frac{y}{I_{mx}} + \frac{I_{xy}}{I_x} - \frac{I_{xy}}{I_y} \sigma \right] \quad (14)$$

In Eq. 1, M corresponds to the bending moment about the orthogonal x-axis at either the mid-span or brace point and I_{mx} and I_{my} are the modified moments of inertia about the x and y axes respectively as defined by Zetlin and Winter (1955))

Torsion Normal Stresses

Normal stresses in the cross section caused by torsion, f_w , are calculated according to the AISC Torsion Analysis Design Guide (Seaburg and Carter, 1997)

$$f_w = E \cdot W_N \cdot (\phi_u'' + \phi_p'' + \phi_{\text{brace}}'') \quad (15)$$

Where W_N is the normalized warping function at a specific point on the cross section and ϕ'' is the second derivative of the rotation function for the applied load with respect to the axis along the span of the beam. The purlin section is subject to three torsion rotation functions: uniform torsion distribution ϕ_u'' , parabolic torsion distribution, ϕ_p'' , and paired concentrated torques, ϕ_{brace}'' . Each rotation function is defined separately for the two critical locations along the span of the purlin: mid-span and brace location.

The rotation functions at the mid-span of the purlin are

$$\phi_u'' = \frac{t_{1st}}{GJ} \left(\frac{1}{\cosh\left(\frac{L}{2a}\right)} - 1 \right) \quad (16)$$

$$\phi_p'' = \frac{t_{2nd}}{GJ} \left[\frac{8a^2}{L^2} \left(1 - \frac{1}{\cosh\left(\frac{L}{2a}\right)} \right) - 1 \right] \quad (17)$$

$$\phi_{brace}'' = \frac{T_{1st} + T_{2nd}}{GJ} \left(\frac{1}{a} \right) \left[\sinh\left(\frac{L}{2a}\right) \left(\frac{\sinh\left(\frac{c}{a}\right) + \sinh\left(\frac{L-c}{a}\right)}{\tanh\left(\frac{L}{a}\right)} - \cosh\left(\frac{L-c}{a}\right) \right) - \cosh\left(\frac{L}{2a}\right) \sinh\left(\frac{c}{a}\right) \right] \quad (18)$$

At the brace location, the rotation functions are:

$$\phi_u'' = \frac{t_{1st}}{GJ} \left(\cosh\left(\frac{c}{a}\right) - \tanh\left(\frac{L}{2a}\right) \sinh\left(\frac{c}{a}\right) - 1 \right) \quad (19)$$

$$\phi_p'' = \frac{t_{2nd}}{GJ} \left[\frac{8a^2}{L^2} \left(\frac{\cosh\left(\frac{L}{a}\right) - 1}{\sinh\left(\frac{L}{a}\right)} \sinh\left(\frac{c}{a}\right) - \cosh\left(\frac{c}{a}\right) + 1 \right) + 4\left(\frac{c}{L}\right)^2 - 4\left(\frac{c}{L}\right) \right] \quad (20)$$

$$\phi_{brace}'' = \frac{T_{1st} + T_{2nd}}{GJ} \left(\frac{1}{a} \right) \sinh\left(\frac{c}{a}\right) \left(\frac{\sinh\left(\frac{c}{a}\right) + \sinh\left(\frac{L-c}{a}\right)}{\tanh\left(\frac{L}{a}\right)} - \cosh\left(\frac{L-c}{a}\right) - \cosh\left(\frac{c}{a}\right) \right) \quad (21)$$

4. Evaluation of real system

To demonstrate the method, 8ZS2.00x0.057 cross sections were analyzed for a uniform load on 0.5:12, 1:12, 2:12, 4:12, 6:12 and 8:12 slopes. The analysis shows that the calculated buckling moment is sensitive to the slope of the system. As the slope of the system increases, the cross section stresses change. By tilting the system from a flat roof to a positive 20°, the bending moment generated on the section increases by the amplitude of 4.5%. From 20 degree to the slope of 50 it goes approximately with zero slopes so the slope of the system in that area does not affect the stresses considerably. Once it reaches the 50° the quantified stresses on the cross section decreased by -4.5%. Since the effect of the tangential component pushes the system back downhill, by increasing the slope after 70° it is added to the torsion effect in the system so the ultimate buckling moment becomes lower than the standard flat roof.

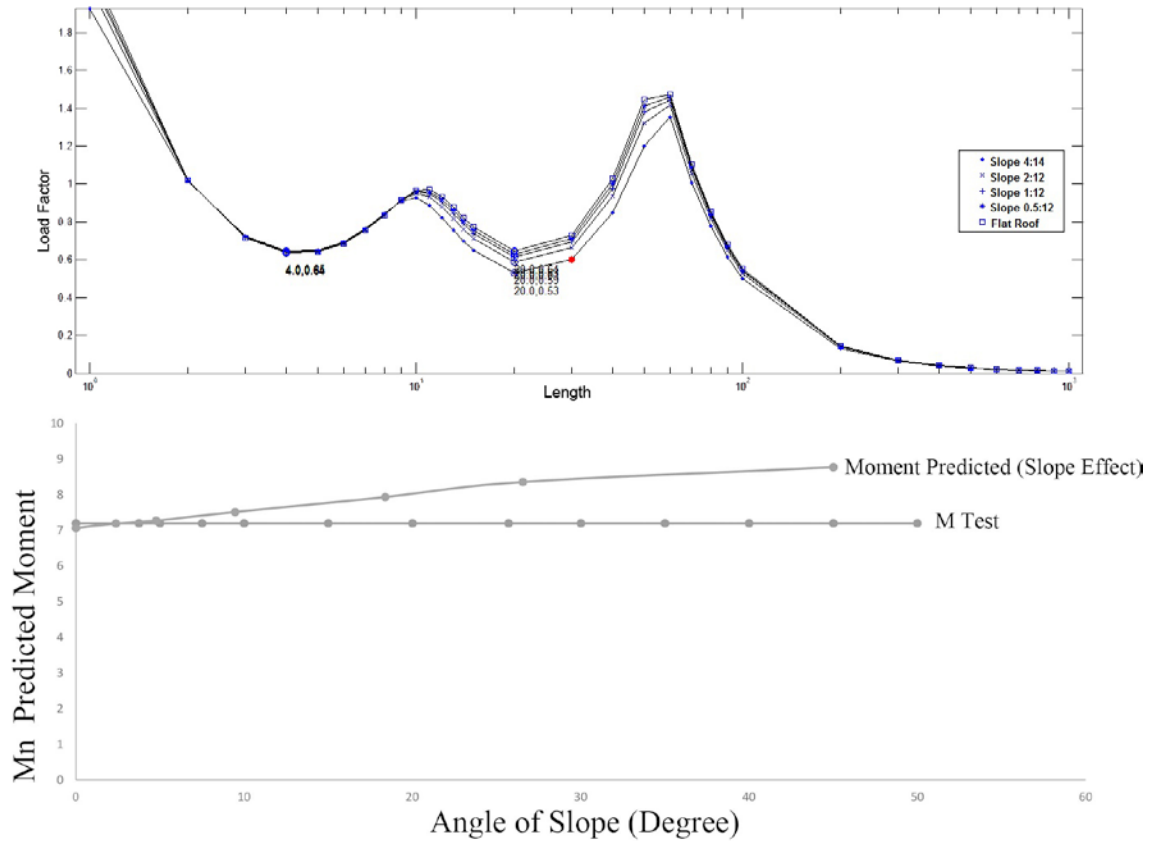


Figure 4. Finite Strip Buckling Analysis (Top)
Predicted Moment Strength vs Roof Slope (Bottom)

Table 1: Bending Moment

Slope	M_{nd} (k-ft)	M_{nl} (k-ft)	M_n (k-ft) predicted	Deflection (inch)
Flat Roof	7.0642	7.8395	7.0642	1.6296
Slope 0.5:12	7.1909	8.0297	7.1909	1.4284
Slope 1:12	7.2702	8.2225	7.2702	1.2254
Slope 2:12	7.5128	8.6101	7.5128	0.8183
Slope 4:12	7.9334	9.4012	7.9334	0.0325
Slope 6:12	8.3555	10.0506	8.3555	-0.9641
Slope 8:12	8.7694	10.5484	8.7694	-1.8293

As it is mentioned in the previous part the system would deflect laterally. The lateral deflection is a function of loading, eccentricity and the slope of the roofing system. By increasing the slope of the system the deflection increases. In figure 5 it shows that with the same pressure on the system, increasing the slope generates fewer deflection in the system. The effect of the slope results on the system in a linear form. While W_x component of the pressure is in the opposite direction that the system tend to deflect the total deflection decreased by going steeper and steeper.

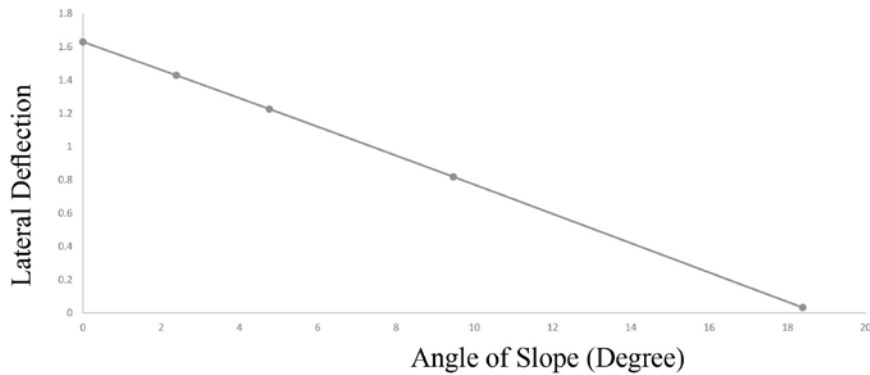


Figure 5. Slope Effect on Lateral Deflection

5. Conclusions

In typical methodology to set up a C- or Z-section purlins that consists of simple span purlins with torsion restraints at paired locations along the length of the member; analyze the strength bending distribution based in constrained condition. The second order effect resists by the pair braces along the span. Several factors affect the amplitude of the stresses created on the structure such as location of the braces, angle of roof slope. With flexible system, the deformations and corresponding stresses in the system on a sloped roof are significantly different on a flat roof.

There is a disconnect between the determination of flexural strength and the evaluation of the bracing. A streamlined procedure to calculate the distribution of forces between the braces and diaphragm is presented that eliminates the discontinuities while expanding the analysis in roof slopes. It also includes imbalances resulting from the standoff effects. To examine the method, lateral deflection and stress distribution of a real scale roof system of standard 8Z16 purlins quantified in different slopes and all data provided. The method shows applicable procedure to design a sloped roof system while considering effects of the standoff and the second order effect.

In Seek (2016) equations provided for paired braces at one third, modified equations for paired braces at any location along the span presented in this paper. To examine the method, stress distribution of a real scale roof system of standard 8Z16 purlins quantified in different slopes. The method shows applicable procedure to design a slope roof system while considering effects of the standoff and the second order effect. Another important aspect of the method is the effects of the slope on the lateral deflection which is crucial in the large roof system. The nonlinear effect of the slope on the lateral deflection developed, the correlation of the predicted results to the stress distribution are very promising.

Acknowledgments

The Authors would like to thank American Iron and Steel Institute and the Metal Building Manufacturers Association for their support of this project through the Small Project Fellowship Program.

References

- AISI (American Iron and Steel Institute). (2013) S908-13 Base Test Method for Purlins Supporting a Standing Seam Roof System. Washington, DC.
- AISI (American Iron and Steel Institute). (2012). North American Specification for the Design of Cold-Formed Steel Structural Members. Washington, DC.
- Seaburg, P. A., Carter, C. J. (1997). *Steel Design Guide Series 9: Torsional Analysis of Structural Steel Members*. American Institute of Steel Construction. Chicago, IL.
- Emde, M. G. (2010) Investigation of Torsional Bracing off Cold-Formed Steel Roofing Systems. Master's Thesis. University of Oklahoma. Norman, OK.
- Li, A., Schafer, B.W. (2010) "Buckling analysis of cold-formed steel members with general boundary conditions using CUFSM: conventional and constrained finite strip methods." Proceedings of the 20th International Specialty Conference on Cold-Formed Steel Structures.
- Murray, T. M., Sears, J., and Seek, M. W. (2009). D111-09 Design Guide for Cold-Formed Steel Purlin Roof Framing Systems. American Iron and Steel Institute. Washington, DC.
- Seek, M. W. (2014). "Improvements to the prediction of brace forces in Z- purlin roof systems with support + third point torsion bracing". Proceedings of the 22nd International Specialty Conference on Cold-Formed Steel Structures.
- Seek, M.W., Ramseyer, C. and Kaplan, I. (2016) "A Combined Direct Analysis and Direct Strength Approach to Predict the Flexural Strength of Z-Purlins with Paired Torsion Braces". Proceedings of the 23rd International Specialty Conference on Cold-Formed Steel Structures.
- Seek, M. W. and McLaughlin, D. (2017) "Impact of clip connection and insulation thickness on bracing of purlins in standing seam roof systems." Conference Proceedings, Structural Stability Research Council Annual Stability Conference. Structural Stability Research Council, University of Missouri-Rolla, Rolla, Missouri.
- Yu, W. and R. A. Laboube. (2010) Cold-Formed Steel Design, 4th ed. John Wiley & Sons. Hoboken, NJ.
- Zetlin, L and G. Winter (1955), "Unsymmetrical Bending of Beams with and without Lateral Bracing." Journal of the Structural Division, ASCE, Vol. 81, 1955.